Plasma spraying of zirconia-reinforced hydroxyapatite composite coatings on titanium

Part II *Dissolution behaviour in simulated body fluid and bonding degradation*

E. CHANG, W. J. CHANG, B. C. WANG, C. Y. YANG*
Departments of Materials Science and Engineering and Orthopaedics, National Cheng-Kung University, Tainan, Taiwan 701*

The change of phase, morphology and bond strength of plasma sprayed hydroxyapatite (HA) coating and ZrO_2/HA composite coatings immersed in simulated body fluid (SBF) for various periods of time was studied. X-ray diffractometry (XRD) and scanning electron microscopy (SEM) were used to identify the phase and observe the morphology of the coating surface before and after immersion. In addition, inductively coupled plasma emission spectroscopy (ICP) was used to measure the ion release rate of coatings in SBF for various periods of time. Observation of the morphology by SEM shows that the composite coating with the addition of ZrO_2 in HA significantly reduced the dissolution rate of impurity phases in simulated body fluid. The argument was supported by measurement of Ca^{2+} ion concentration in SBF. During plasma spraying, less OH^- ions were lost in a ZrO_2-containing composite coating. This factor, together with the reduced effective surface of the ZrO_2-containing HA coating, were attributed to the reduced dissolution rate of the composite coatings. All the plasma sprayed coatings degraded after immersion in SBF owing to dissolution of constituents in the coating, however, the addition of ZrO_2 in HA improved the bonding strength of HA coating after immersion in SBF.

1. Introduction

Hydroxyapatite (HA) has received increasing attention as a bone implant material to promote fixation of orthopaedic prostheses. *In vitro* and *in vivo* tests on plasma-sprayed hydroxyapatite coated titanium implants have shown that the thin layer of HA coating (HAC) promotes direct chemical bonding with bone [1, 2] and exhibits bone apposition and satisfactory biocompatibility [3–6]. Despite this, the long-term strength and fracture toughness of HA and HAC has been questioned [3, 7]. The poor bonding strength of HAC is attributed to the following causes: (1) inadequate bonding between HAC and the substrate; and (2) inadequate strength of HA or inter lamellar layers of HA *per se*. For the former cause, the concept of a bond coat to provide a mechanical or chemical bond between HAC and the bond coat can be exercised, and for the latter the plasma coating can be reinforced by a second phase [7, 8]. Zirconia, having the attributes of high strength and stress-induced phase transformation toughening, is a candidate material to strengthen the ceramics [9–11]. In a previous paper, it was proved that the addition of yittria-stabilized zirconia improved the bonding of hydroxyapatite coatings to titanium [12]. Continuing the previous investigation, the present work aims to investigate the effect of zirconia on the bonding at the HAC/Ti alloy interface as a function of the period of immersion in simulated body fluid (SBF).

2. Materials and methods

2.1. Specimens preparation

As described previously [12], four kinds of plasma spray powders of the following compositions were prepared: HA, HA + 5 wt% TZ3Y (3–5), HA + 10 wt % TZ3Y (3–10), and HA + 10 wt % TZ8Y (8–10), where TZ3Y and TZ8Y denote ZrO_2–3 mol % Y_2O_3 and ZrO_2–8 mol % Y_2O_3, respectively. The granulated powders, sintered at 600 °C for 1 h and 1000 °C for 4 h, have a size distribution of − 120– + 200 mesh (74–125 μm). Two shapes of Ti-6Al-4V (ASTM F-136) were used as substrate: plate specimens measuring $1 \times 1 \times 0.3$ cm were used for microstructure and phase analyses, and cylindrical rods measuring 2.54 cm in diameter and 7.62 cm in length for bonding strength measurements. The prepared powders were plasma sprayed onto the ultrasonically cleaned and sand blasted surface before plasma spraying with the parameters as stated previously [12]. The coating thickness was about 200 μm.

0957–4530

TABLE I Concentration of ions in simulated body fluid [13]

Ion	Na^+	K^+	Ca^{2+}	Mg^{2+}	Cl^-	HCO_3^-	HPO_4^{2-}
Concentration (MM)	142.0	5.0	2.5	1.5	148.8	4.2	1.0

2.2. Change of HA and ZrO_2/HA composites after immersion

The plasma-sprayed plate specimens were ultrasonically cleaned in acetone, rinsed in distilled water and then inserted into dry heat (120 °C × 8 h) sterilized culture vials containing simulated body fluid. The compositions of SBF, shown in Table I, was buffered at pH of 7.2 with 50 mM tris-hydroxymethyl-aminomethane and 45 mM HCl [13]. The specimen surface to SBF ratio was 1 cm^2 : 1 m*l*, and the temperature of SBF was kept at 36.5 °C. The as-sprayed specimens, together with specimens removed from SBF after 1, 2, 5, 10 and 20 days, were examined for variation of coating characteristics. The phase identity from the coating surface of as-sprayed and after-immersion specimens was examined by X-ray diffractometry (XRD) (Rigaku D/Max III, V) with a scan speed of 4°/min between 20° and 60° (2θ angle) using CuK_α radiation. A scanning electron microscope (SEM) equipped with wavelength dispersive spectrometer (WDS) was used to observe the morphology change and examine the Zr element of the coating surface before and after immersion. In addition, inductively coupled plasma emission spectroscopy (ICP) (Kontron Plasmakon model S-35) was used to measure the ion release rate of coatings in SBF over various periods of time.

2.3. Adhesion test at HA and ZrO_2/HA composites/Ti interface

The plasma-sprayed specimens were used to investigate the changes in bonding strength before and after immersed in SBF. For as-sprayed specimens, the testing procedures for bond strength has been previously described [12]. For immersed rod specimens, the soaking sequences used were similar to those for plate specimens as described above. The bond strength at the HA or ZrO_2/HA composite /Ti-6Al-4V interface was also tested using the adhesion test per ASTM C-633. After 1, 2, 5, 10 and 20 days of immersion, the HA and ZrO_2/HA composite coating rods were removed, washed with distilled water and dried in oven and then adhered to grit blasted loading rods using an adhesion bonding glue (METCO EP-15). The couples cured at 190 °C for 2 h were subjected to tensile tests at an extension rate of 0.02 mm/s until failure. For each testing material, five specimens were used, and the bonding strength data is reported as the average values.

3. Results and discussion

The results of XRD analysis of HA coating and HA + 10 wt % TZ8Y (8–10), HA + 5 wt % TZ3Y (3–5) and HA + 10 wt % TZ3Y (3–10) composite coatings, immersed in simulated body fluid for 0, 1, 2, 5, 10 and 20 days, are shown in Figs. 1, 2, 3 and 4, respectively. Observation of the HA coating, as shown in Fig. 1, reveals that impurity phases such as $Ca_3(PO_4)_2$ (or TCP), $Ca_4P_2O_9$ and CaO disappeared gradually

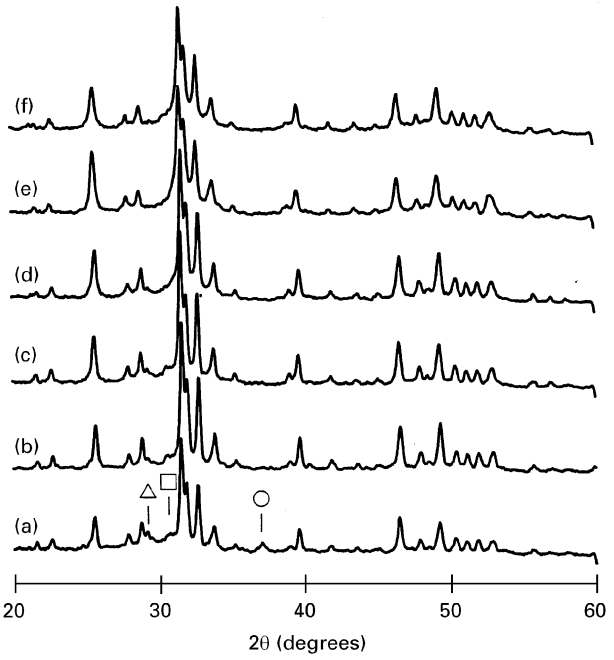

Figure 1 XRD analyses of HA coating immersed in SBF for (a) 0, (b) 1, (c) 2, (d) 5, (e) 10 and (f) 20 days. △ $Ca_4P_2O_9$; □ TCP; ○ CaO.

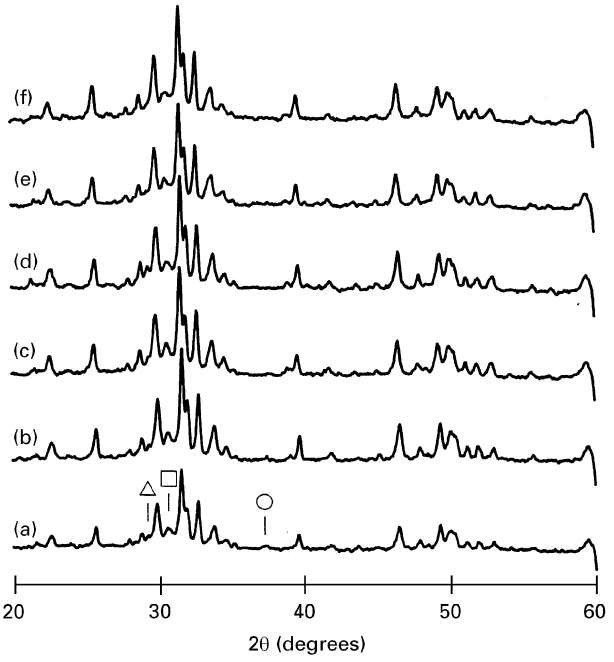

Figure 2 XRD analyses of 8–10 coating immersed in SBF for (a) 0, (b) 1, (c) 2, (d) 5, (e) 10 and (f) 20 days. △ $Ca_4P_2O_9$; □ TCP; ○ CaO.

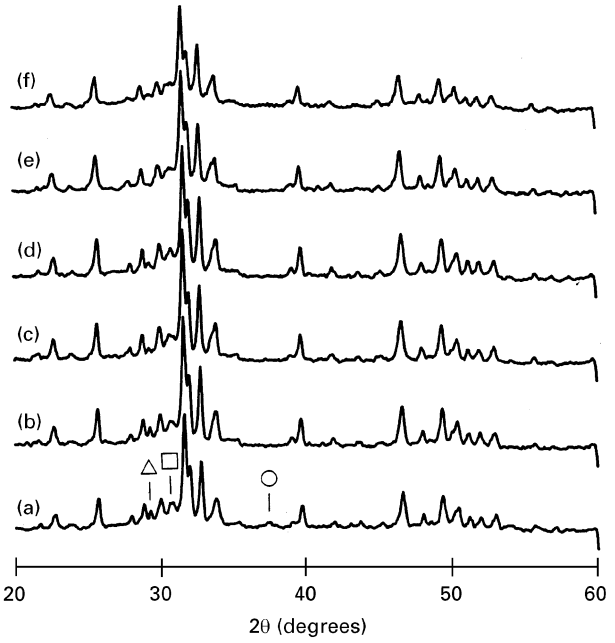

Figure 3 XRD analyses of 3–5 coating immersed in SBF for (a) 0, (b) 1, (c) 2, (d) 5, (e) 10 and (f) 20 days. △ $Ca_4P_2O_9$; □ TCP; ○ CaO.

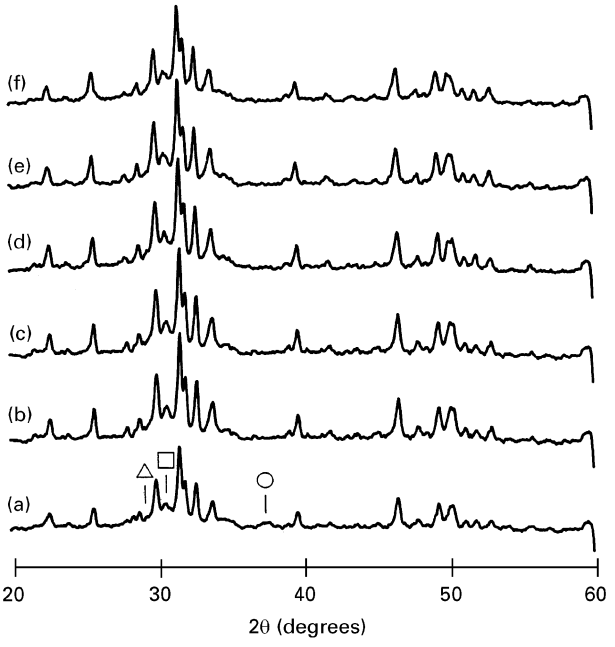

Figure 4 XRD analyses of 3–10 coating immersed in SBF for (a) 0, (b) 1, (c) 2, (d) 5, (e) 10 and (f) 20 days. △ $Ca_4P_2O_9$; □ TCP; ○ CaO.

as the period of immersion increased; e.g. CaO dissolved after 1 day, and TCP and $Ca_4P_2O_9$ dissolved after 10 days. The performance of the 8–10 composite coating (Fig. 2) is slightly different from the HA coating in that the dissolution rate of impurity phases was slower. As indicated in this figure, the CaO impurity phase disappeared only after 2 days, and residual $Ca_4P_2O_9$ remained after 20 days; special attention should be paid to the TCP impurity phase of which the intensity was similar to the composite before immersion. The argument is confirmed in Table II which shows the integration intensity (in arbitrary units) of the TCP phase of the 8–10 specimen. The dissolution of 3–5 and 3–10 coatings resembles that of the 8–10 coating as indicated in Figs. 3 and 4.

TABLE II XRD diffraction intensity (in arbitrary units) of TCP phase of the 8–10 specimen as a function of time in SBF

Time (days)	0	1	2	5	10	20
TCP intensity	232.8	227.7	209.4	200.3	189.6	200.7

The SEM surface morphologies of the HA coating and 8–10, 3–5 and 3–10 composite coatings before and after immersion in simulated body fluid for various periods of time are shown in Figs. 5, 6, 7 and 8, respectively. Examination of the HA coating, as indicated in Fig. 5, shows that the constituents on the surface were partially dissolved after 2 days (as indicated by the arrow in Fig. 5c). The dissolution became severe as the period increased, and the surface of the coating became flat after 20 days of immersion in SBF (Fig. 5f). The results of dissolution from observation of surface morphologies are apparently consistent with the findings from the XRD analyses, namely that the impurity phases in the HA coating dissolved steadily with time into the SBF. The display of the ZrO_2-containing 8–10 composite coating (Fig. 6) is significantly different from that of the HA coating, and the coating underwent little apparent change of morphology after 20 days of immersion. The morphological examination supports the previous XRD measurements concerning the dissolution of impurity phases in the 8–10 composite coating. Figs. 7 and 8 show that the evolution of morphology with time for the 3–5 and 3–10 ZrO_2-containing coatings can be catagorized with the 8–10 coating.

Fig. 9 shows the ICP chemical analysis of the calcium ion concentration in simulated body fluid for the HA coating and for 8–10, 3–5 and 3–10 composite coatings after 0, 1, 2, 5, 10 and 20 days. During initial periods of immersion, the calcium ion increased rapidly in the SBF owing to the higher content of more soluble impurity phases in the coatings [14]; thereafter the dissolution rate decreased and the concentration of Ca^{2+} came to a steady state value. The ZrO_2-containing coatings exhibit similar trends to the HA coatings, but the kinetics of dissolution were more moderate and it took a much longer time for the dissolution of impurity phases to take place.

In general, various causes, such as phase, crystallinity, grain size, porosity, specific area and thickness of materials might affect the dissolution of ions in bioceramics [15]. The factors that affect the dissolution of HA due to the addition of ZrO_2 are qualitatively analysed as follows.

(1) *Phases*: Addition of ZrO_2 increased the impurity phases significantly as described previously [12], and these phases dissolve faster than HA [14]. Therefore, the fact that composite coatings degraded slower than the HAC, as shown by comparing Figs. 1–9 in this work, cannot be rationalized by the higher content of impurity phases. Secondly, ZrO_2 accounts for 5 to 10 wt % in the composite coatings, and this phase does

not dissolve in SBF; with an increased ZrO_2 content 3–10 dissolved slower than the 3–5 specimen, as indicated in Fig. 9. Yet the explanation is complicated by the affect of ZrO_2 on the OH^- ions associated with the stretching mode at $3570\,cm^{-1}$ [14] detected by FTIR spectrometry (FTIR Nicolet 800). After plasma spraying, the OH^- ions remaining in ZrO_2-containing hydroxyapatite coatings were shown to be more numerous than in pure HA coating, as measured by FTIR in Fig. 10, but the reason for this was not understood. Since HA becomes more soluble as more OH^- ions are lost [16], the slower dissolution behaviour of the composite coatings might also be explained by their ability to preserve OH^- ions during plasma spraying.

(2) *Porosity*: Since the addition of ZrO_2 induces more porosity in the composite coatings [12], and porosity in the coating will accelerate dissolution,

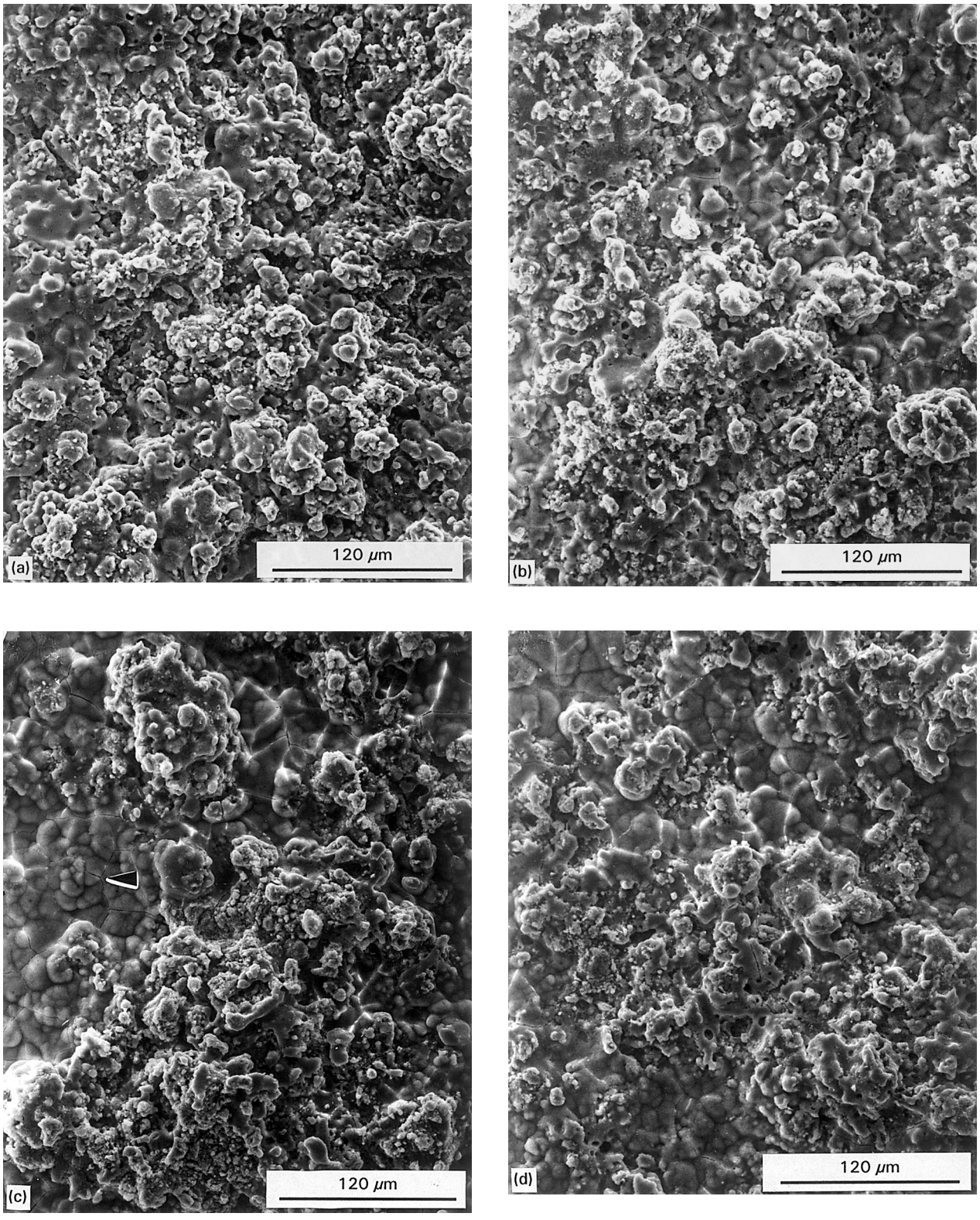

Figure 5 Morphology of HA coating immersed in SBF for (a) 0, (b) 1, (c) 2, (d) 5, (e) 10 and (f) 20 days.

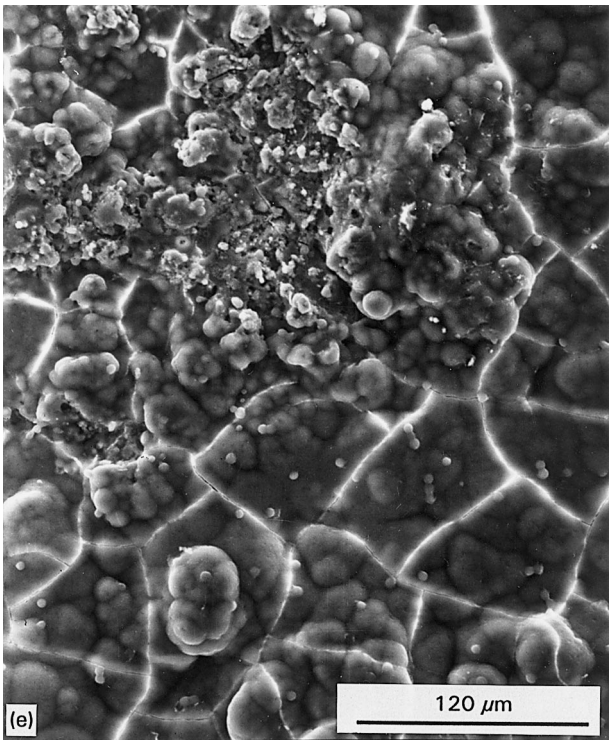

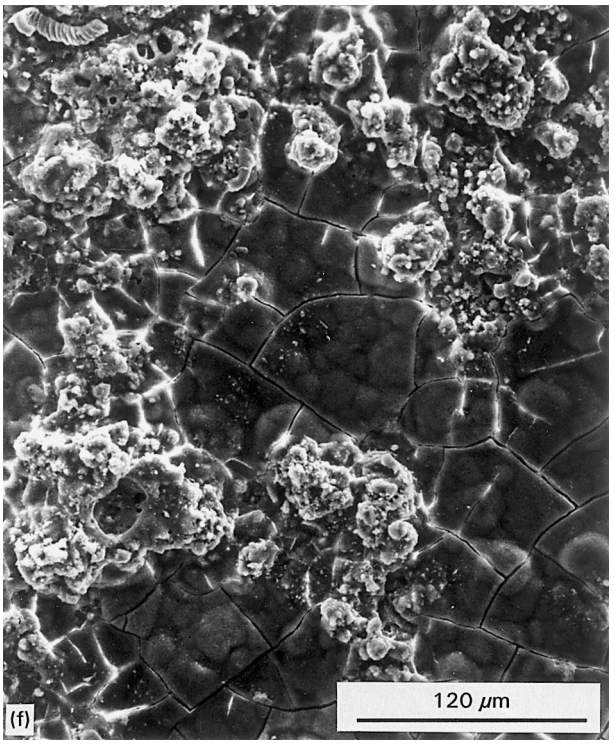

Figure 5 (Continued)

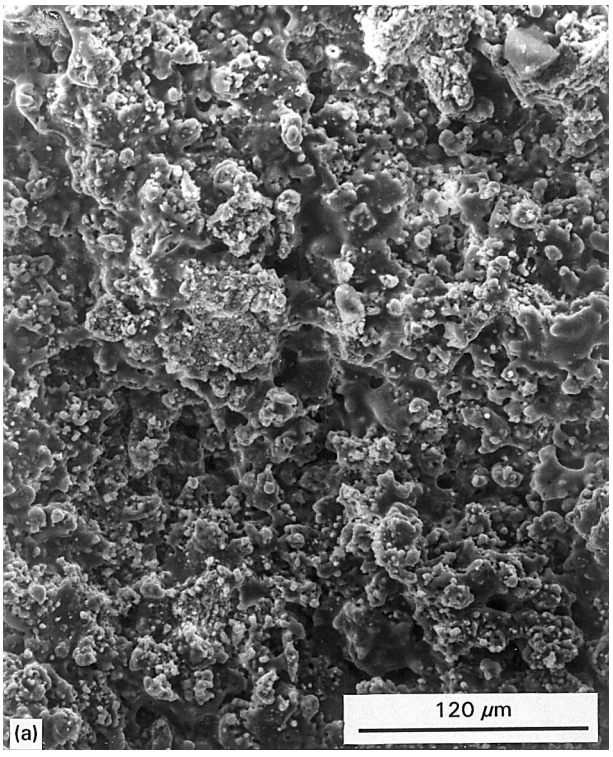

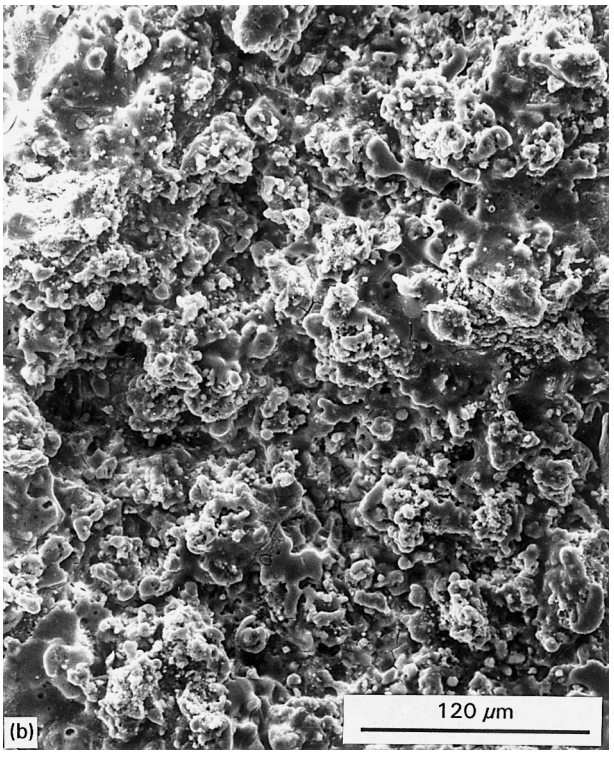

Figure 6 Morphology of 8–10 coating immersed in SBF for (a) 0, (b) 1, (c) 2, (d) 5, (e) 10 and (f) 20 days.

the slower dissolution rate of ZrO_2-containing hydroxyapatite coatings cannot be attributed to the variation of porosity content.

(3) *Effective HA surface*: As HA dissolves, the undissolved ZrO_2 remaining on the coating may hinder contact between the HA and the SBF, which in turn will reduce the dissolution rate of ZrO_2-containing hydroxyapatite coatings. Fig. 11 shows the WDS analysis of the variation of Zr on the surface of coatings after various periods of immersion in SBF; it is indicated that Zr increased rapidly on the surface of coatings, and this is thought to be a factor which hindered contact between HA and SBF and reduced the dissolution kinetics.

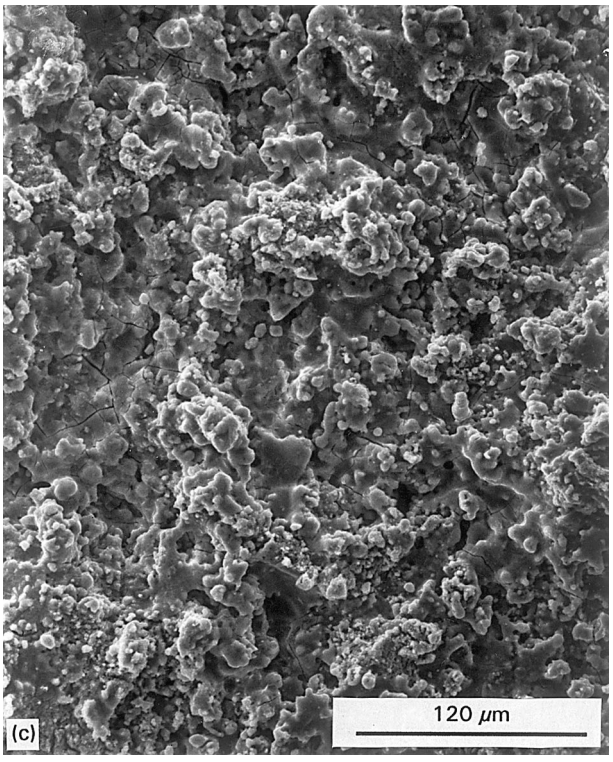

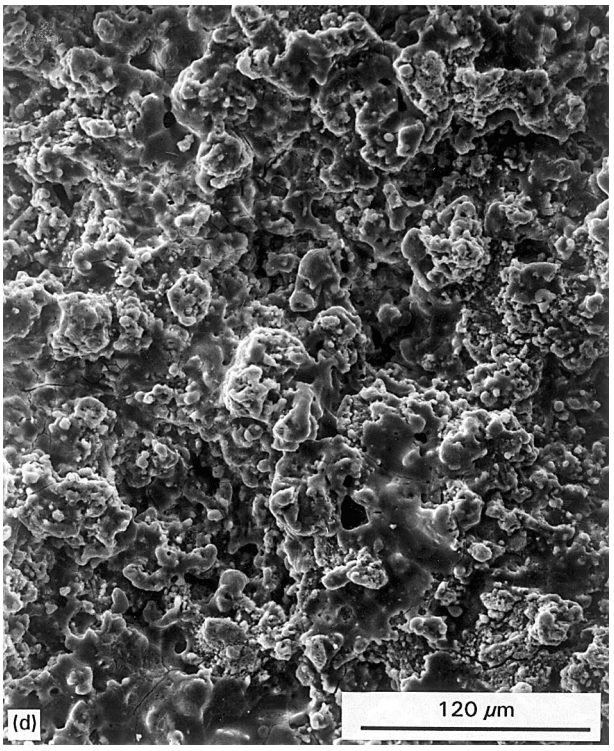

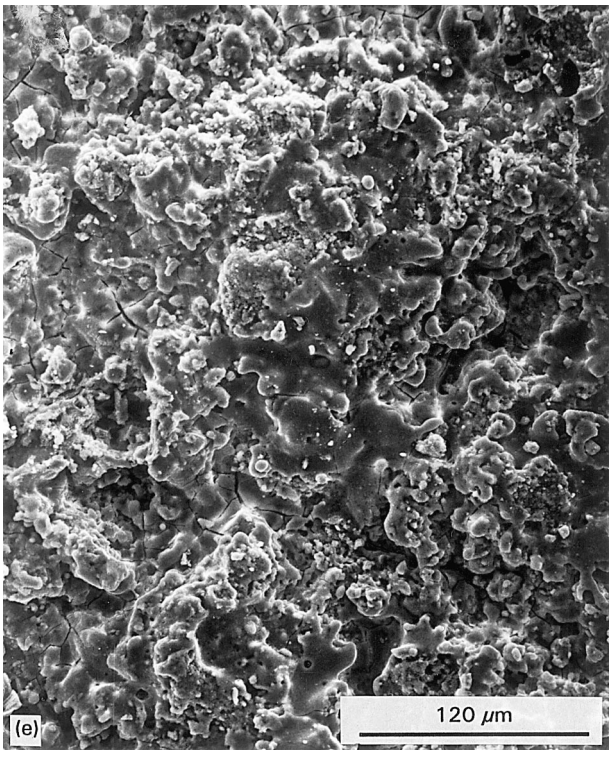

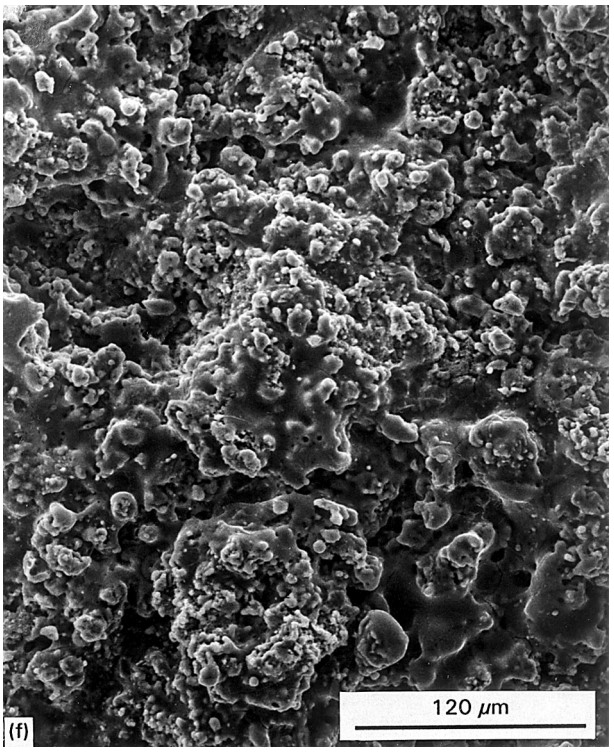

Figure 6 (continued).

The quantitative contribution of the various factors to the dissolution of HA as affected by ZrO_2 cannot be established from this study. However, the factors leading to retardation of the dissolution as affected by ZrO_2 obviously dominates. Moreover, other factors not discussed above may not be excluded.

After SBF immersion, the variation of bonding strength with time is shown in Table III and Fig. 12, which indicate that the bonding strength decays with time. The bonding strength reached minimum values after 5 days and increased slightly thereafter. The decay of bonding strength is caused by the dissolution of coatings which weakens them. The minimum in bonding strength corresponds to saturation of Ca^{2+} concentration which occurred after 5 days, as shown in Fig. 9. Dissolution of constituents inside the coatings reduces the cohesive strength of the coatings. Yang *et al.* studied the *in vitro* bond degradation at the

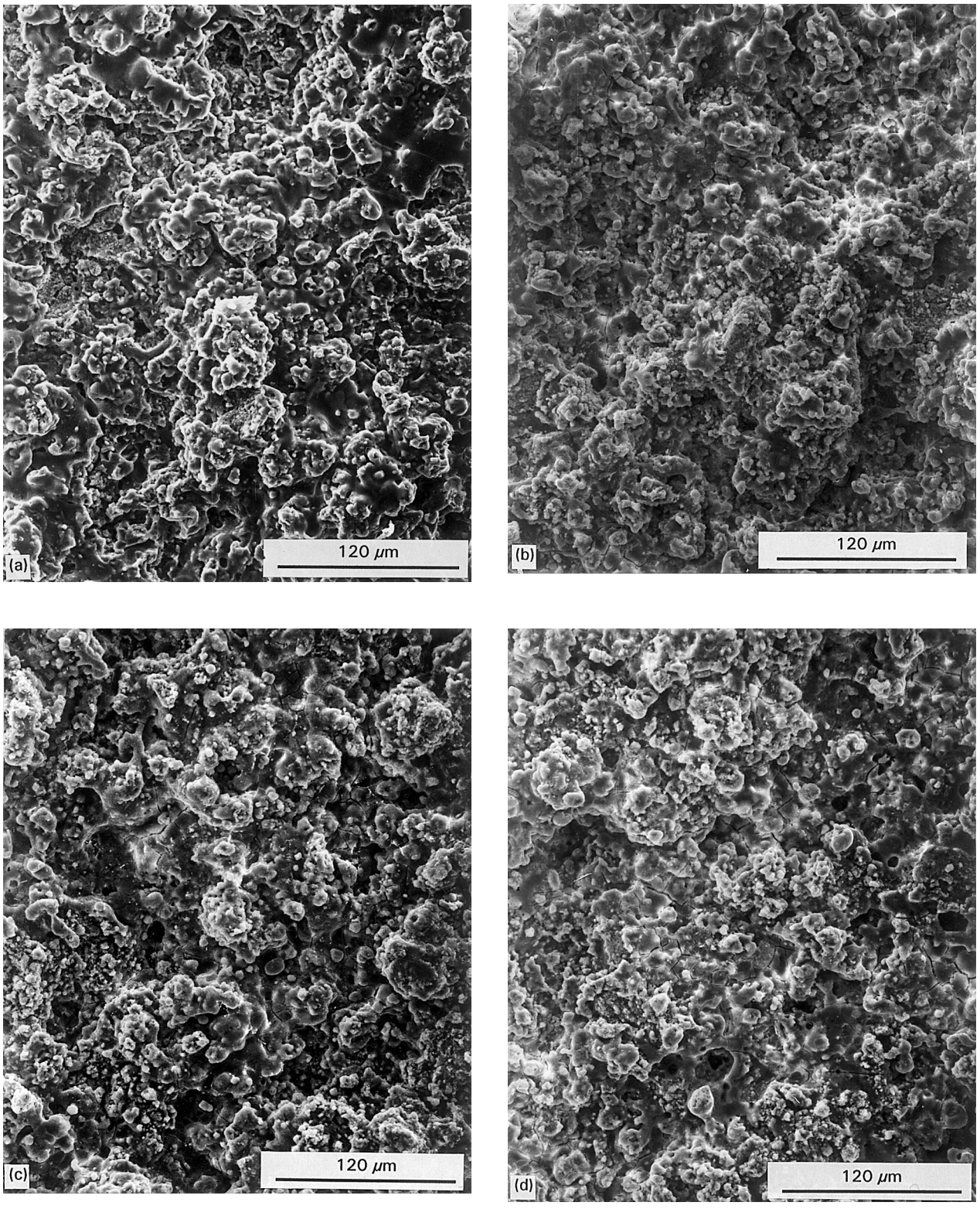

Figure 7 Morphology of 3–5 coating immersed in SBF for (a) 0, (b) 1, (c) 2, (d) 5, (e) 10 and (f) 20 days.

plasma-sprayed HA coating/Ti-6Al-4V alloy interface and found that the bonding strength increased after decreasing to a minimum [17]. The bond recovery phenomenon was attributed to the penetration of glue into cavities in the dissolved coating, which artificially strengthens the coating. In the present work, a slight recovery of bond degradation was also observed.

As bond decay corresponds to the dissolution of the coating, fast dissolution of the coating will result in more bonding decay at the HA or ZrO_2/HA composite coatings/Ti-6Al-4V interface. Of the four coatings investigated in this study, the HA coating dissolved fastest and hence the bond also decayed proportionally. After SBF immersion for 1 day, as shown in Fig. 12, the bonding strength of the HA coating decreased from 28.2 MPa to 19.7 MPa, while in comparison, the bond strength of the 8–10 specimen decreased from 32.5 MPa to 25.3 MPa. The

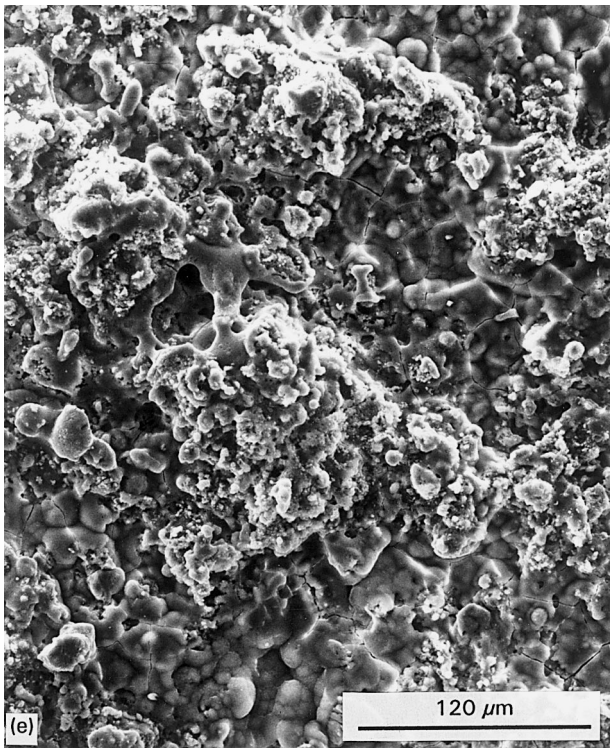

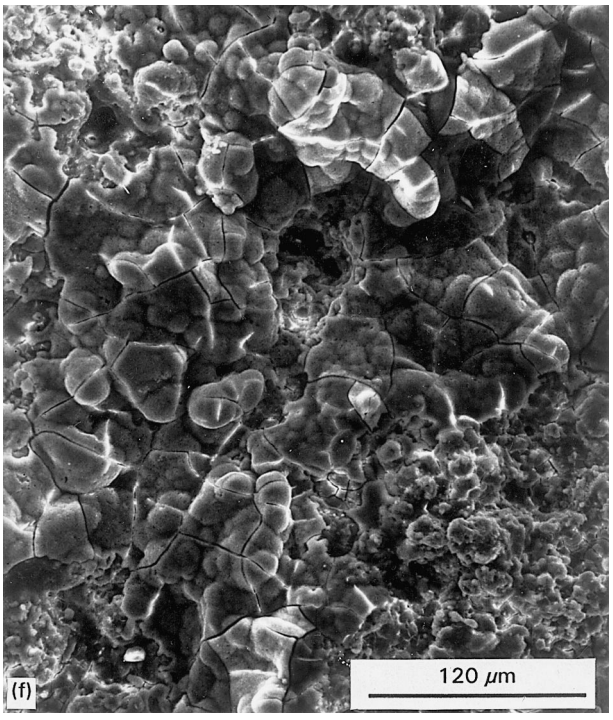

Figure 7 (continued)

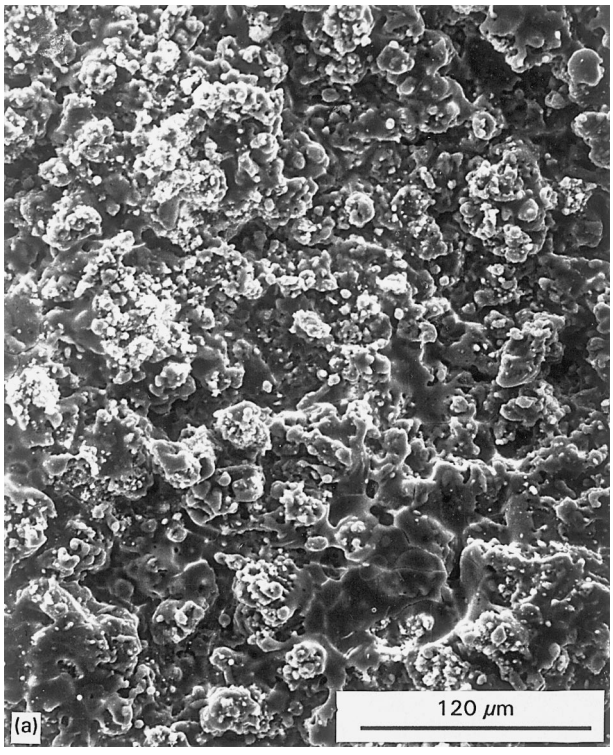

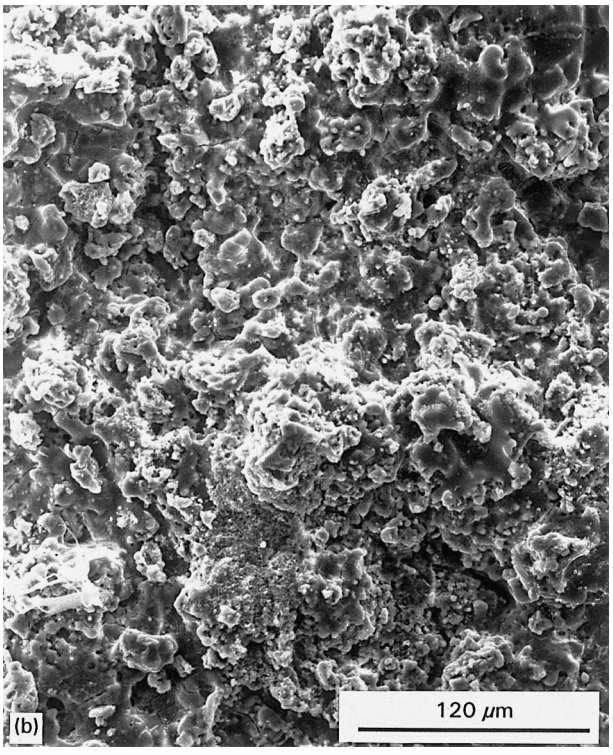

Figure 8 Morphology of 3–10 coating immersed in SBF for (a) 0, (b) 1, (c) 2, (d) 5, (e) 10 and (f) 20 days.

decay became more evident after 2 days for the HA coating. The slower bond decay of ZrO_2-containing hydroxyapatite coatings is explained by the slower dissolution rate as discussed above. After soaking for 20 days, bond recovery occurred in the HA and 3–5 coatings, as shown in Fig. 12, corresponding to the higher dissolution rates of these coatings as suggested in Fig. 9; the bonding strength measurements at 20 days for the HA and 3–5 coatings are considered invalid tests.

4. Conclusions

The dissolution behaviour in simulated body fluid and the bonding degradation of plasma-sprayed

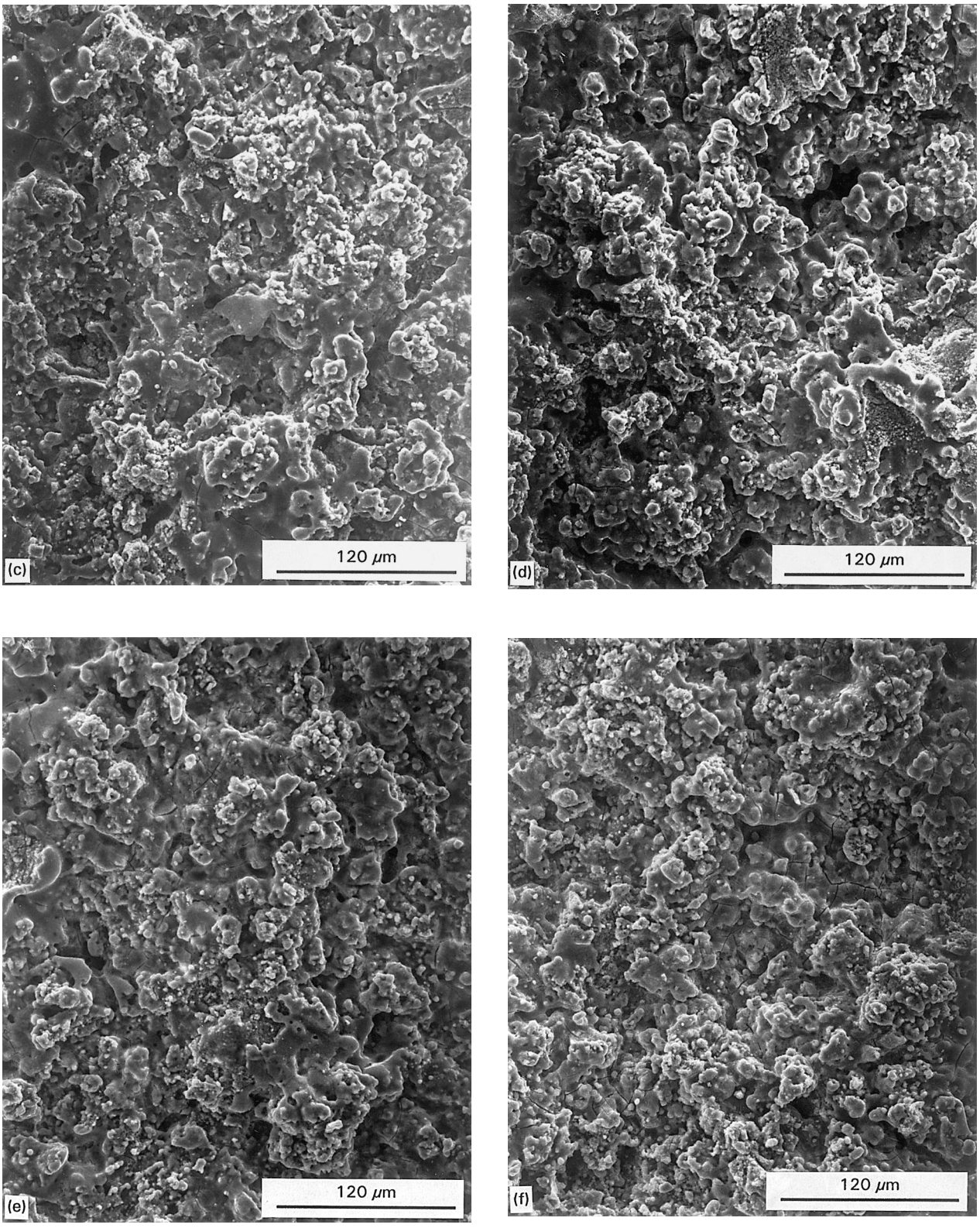

Figure 8 (continued)

hydroxyapatite coating and zirconia-reinforced hydroxyapatite composite coatings was studied. Observation by XRD and SEM techniques shows that the dissolution rate of the ZrO_2/HA composite coatings was slower than that of pure HA coating in simulated body fluid. Measurement of the concentration of Ca^{2+} ions in simulated body fluid confirms the argument. Although the addition of ZrO_2 increased the impurity phases and porosity in the composite coating, which should accelerate dissolution, factors such as less loss of OH^- ions during plasma spraying and the reduced effective surface of HA dominated the dissolution rate. Regarding bond degradation, all the plasma sprayed coatings degraded after immersion in simulated body fluid owing to the dissolution of constituents in the coating, however, the bonding strength of ZrO_2-containing coatings was superior to HA coatings for all periods of immersion in simulated body fluid.

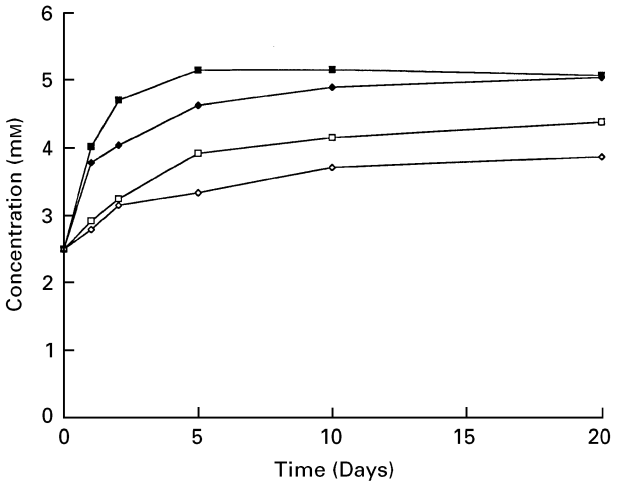

Figure 9 ICP analysis of the variation of Ca^{2+} ions in SBF as a function of time; ■HA. □ 8–10; ◆ 3–5; ◇ 3–10.

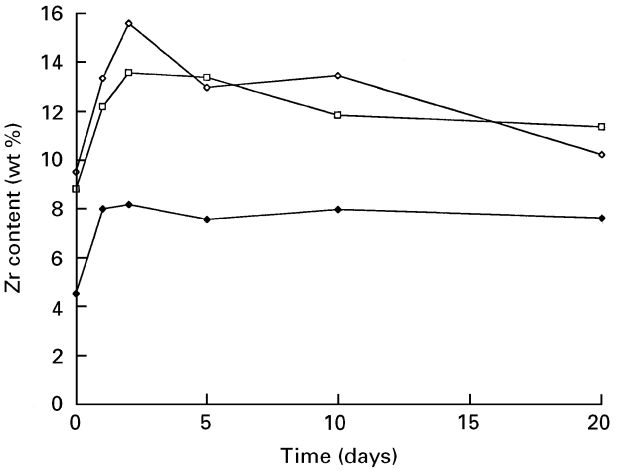

Figure 11 WDS analysis of the variation of Zr on the surface of varoius coatings as a function of time immersed in SBF. □ 8–10; ◆ 3–5; ◇ 3–10.

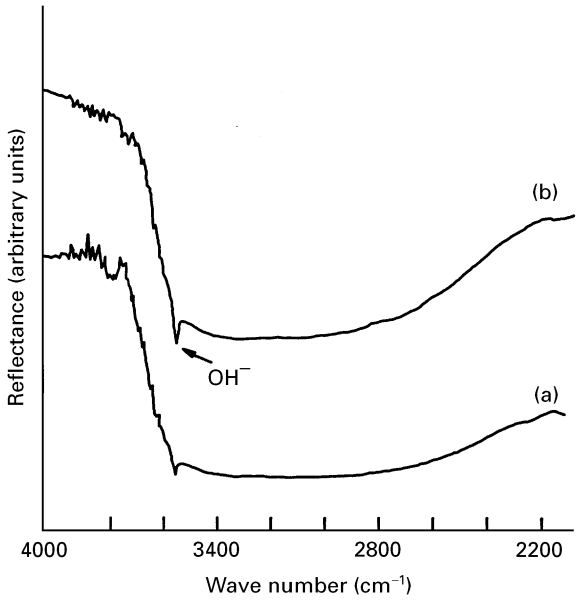

Figure 10 FTIR spectra of (a) HA and (b) 8–10 coating.

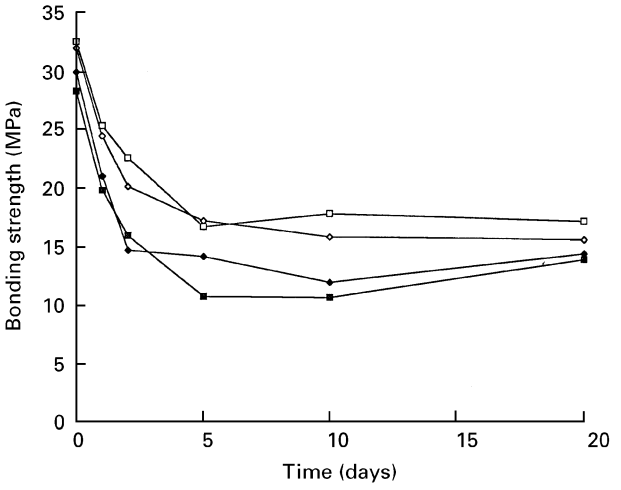

Figure 12 Variation of bonding strength of various coatings as a function of time immersed in SBF. ■HA; □ 8–10; ◆ 3–5; ◇ 3–10.

TABLE III Bonding strength of HA coating and 8–10, 3–5 and 3–10 ZrO_2/HA coatings as a function of time in SBF

Coating	Bond strength (MPa) after period of immersion (days) of 0	1	2	5	10	20
HA	28.2 ± 3.7	19.8 ± 2.2	15.9 ± 4.2	10.8 ± 2.6	10.7 ± 2.4	13.9 ± 3.2
8–10	32.5 ± 4.2	25.3 ± 4.1	22.6 ± 1.2	16.7 ± 4.4	17.8 ± 1.7	17.2 ± 4.6
3–5	29.9 ± 2.5	21.0 ± 1.6	14.7 ± 3.8	14.2 ± 1.5	12.0 ± 2.9	14.4 ± 2.9
3–10	32.0 ± 3.3	24.4 ± 2.9	20.1 ± 3.2	17.2 ± 4.4	15.8 ± 2.2	15.6 ± 3.2

References

1. R. G. T. GEESINK, K. DE GROOT and P. A. T. CHRISTEL, *Clin. Orthop.* **225** (1987) 147.
2. R. G. T. GEESINK, K. DE GROOT and C. P. A. KLEIN, *J. Bone Joint Surg.* **70B** (1988) 17.
3. K. DE GROOT, R. GEESINK, C. P. A. T. KLEIN and P. SEREKIAN, *J. Biomed. Mater. Res.* **21** (1987) 1375.
4. K. HAYASHI, K. UENOYAMA, N. MATSUGUCHI, Y. SUGIKA, *ibid.* **25** (1991) 515.
5. J. A. JANSEN, J. P. C. M. VAN DE WAERDEN, J. G. C. WOLKE and K. DE GROOT, *ibid.* **25** (1991) 973.
6. B.C. WANG, E. CHANG, D. TU and C. Y. YANG, *J. Mater. Sci. Mater. Med.* **4** (1993) 394.
7. C. C. BERNDT and J. H. YI, *Mater. Sci. Forum* **34–36** (1988) 469.
8. C. C. BERNDT and J. H. YI, *Surf. Coat. Technol.* **37** (1989) 89.
9. Y. MURASE, E. KATO and K. DAIMON, *J. Amer. Ceram. Soc.* **69** (1986) 83.

10. S. R. WITEK and E. D. BUTLER, *J. Mater. Sci. Lett.* **4** (1985) 1412.
11. Q. L. GE, T. C. LEI and Y. ZHOU, *Mater. Sci. Technol.* **7** (1991) 490.
12. E. CHANG, W. J. CHANG, B. C. WANG and C. Y. YANG, *J. Mater. Sci. Mater. Med.* **8** (1997)
13. T. KOKUBO, in "CRC handbook of bioactive ceramics", Vol. I, edited by T. Yamamuro, L. L. Hench and J. Wilson (CRC Press, Florida, 1990) p. 41.
14. J. D. HAMAN, L. C. LUCAS and D. CRAWMER, *Biomaterials* **16** (1995) 229.
15. P. DUCHEYNE and J. F. McGUCKIN, JR, in "CRC handbook of bioactive ceramics", Vol. II, edited by T. Yamamuro, L. L. Hench and J. Wilson (CRC Press, Florida, 1990) p. 175.
16. P. DUCHEYNE, S. RADIN and L. KING, *J. Biomed. Mater. Res.* **27** (1993) 25.
17. C. Y. YANG, B. C. WANG, E. CHANG and B. C. WU, *J. Mater. Sci. Mater. Med.* **6** (1995) 258.

Received 6 February
and accepted 14 March 1996